ADVANCING EARTH AND SPACE SCIENCES

Geophysical Research Letters

RESEARCH LETTER
10.1029/2023GL104914

Extreme Altitudes of Stratospheric Hydration by Midlatitude Convection Observed During the DCOTSS Field Campaign

Cameron R. Homeyer[1], Jessica B. Smith[2], Kristopher M. Bedka[3], Kenneth P. Bowman[4], David M. Wilmouth[2], Rei Ueyama[5], Jonathan M. Dean-Day[6], Jason M. St. Clair[7,8], Reem Hannun[9], Jennifer Hare[2], Apoorva Pandey[2], David S. Sayres[2], Thomas F. Hanisco[7], Andrea E. Gordon[1], and Emily N. Tinney[1]

[1]School of Meteorology, University of Oklahoma, Norman, OK, USA, [2]Harvard John A. Paulson School of Engineering and Applied Sciences, Harvard University, Cambridge, MA, USA, [3]NASA Langley Research Center, Hampton, VA, USA, [4]Department of Atmospheric Sciences, Texas A&M University, College Station, TX, USA, [5]NASA Ames Research Center, Moffett Field, CA, USA, [6]Bay Area Environmental Research Institute, Moffett Field, CA, USA, [7]NASA Goddard Space Flight Center, Greenbelt, MD, USA, [8]University of Maryland Baltimore County, Baltimore, MD, USA, [9]Department of Geology & Environmental Science, University of Pittsburgh, Pittsburgh, PA, USA

Key Points:

- Tropopause-overshooting convection in the United States hydrates the stratosphere to exceptional heights
- Observations of the height of stratospheric convective hydration during the Dynamics and Chemistry of the Summer Stratosphere field campaign exceed all prior global records
- The overworld stratosphere is routinely hydrated by midlatitude overshooting convection

Supporting Information:

Supporting Information may be found in the online version of this article.

Correspondence to:

C. R. Homeyer,
chomeyer@ou.edu

Citation:

Homeyer, C. R., Smith, J. B., Bedka, K. M., Bowman, K. P., Wilmouth, D. M., Ueyama, R., et al. (2023). Extreme altitudes of stratospheric hydration by midlatitude convection observed during the DCOTSS field campaign. *Geophysical Research Letters*, *50*, e2023GL104914. https://doi.org/10.1029/2023GL104914

Received 9 JUN 2023
Accepted 22 AUG 2023

Author Contributions:

Conceptualization: Cameron R. Homeyer
Data curation: Cameron R. Homeyer, Jessica B. Smith, Kristopher M. Bedka, Rei Ueyama, Jonathan M. Dean-Day, Jason M. St. Clair, Reem Hannun, Jennifer Hare, Apoorva Pandey, David S. Sayres, Thomas F. Hanisco
Formal analysis: Cameron R. Homeyer

Abstract

Water vapor's contribution to Earth's radiative forcing is most sensitive to changes in its lower stratosphere concentration. One recognized pathway for rapid increases in stratospheric water vapor is tropopause-overshooting convection. Since this pathway has been rarely sampled, the NASA Dynamics and Chemistry of the Summer Stratosphere (DCOTSS) field project focused on obtaining in situ observations of stratospheric air recently affected by convection over the United States. This study reports on the extreme altitudes to which convective hydration was observed. The data show that the overworld stratosphere is routinely hydrated by convection and that past documented records of stratospheric heights of convective hydration were exceeded during several DCOTSS flights. The most extreme event sampled is highlighted, for which stratospheric water vapor was increased by up to 26% at an altitude of 19.25 km, a potential temperature of 463 K, and an ozone mixing ratio >1500 ppbv.

Plain Language Summary

When thunderstorms reach into the second layer of the atmosphere above Earth's surface, the stratosphere, they may impact the concentration and distribution of trace gases that are important to chemistry and climate. One gas that is routinely affected during these events is water vapor, which is typically scarce in the stratosphere. This study presents new aircraft observations of extreme heights in the stratosphere moistened by these thunderstorms. Since increases in stratospheric water vapor positively contribute to warming of Earth's climate and can activate chemistry that destroys ozone, better understanding of this phenomenon helps refine our understanding of its role in the climate system. The new aircraft observations provide clear evidence that water vapor is enhanced by thunderstorms at higher levels in the stratosphere than previously recognized.

1. Introduction

Water vapor (H_2O) is a greenhouse gas that contributes significantly to Earth's radiative forcing in the troposphere and stratosphere. Increases in H_2O concentration lead to increased warming of the climate system, with large sensitivity to concentration changes in the lower stratosphere (LS), especially in the midlatitudes (Banerjee et al., 2019; Forster & Shine, 1999; S. Solomon et al., 2010). While stratospheric H_2O is globally constrained by the tropical tropopause temperature via vertical transport by the Brewer-Dobson circulation and production from methane oxidation (Brewer, 1949; Le Texier et al., 1988), processes that rapidly transport air and condensed water (ice) upward across the tropopause also impact LS H_2O. Extremes in LS H_2O are commonly driven by two processes: moist convection (thunderstorms; Schwartz et al., 2013) and volcanic eruptions (Millán et al., 2022). While stratosphere-impacting volcanic eruptions are intermittent and largely unpredictable, tropopause-overshooting convection occurs routinely in many regions and may increase in frequency as the climate warms (Del Genio et al., 2007; Gensini & Mote, 2015; Romps et al., 2014). Overshooting convection generated by fires (pyroconvection)—a unique compound event—has also received increasing attention as a source for LS H_2O in recent years (S. Khaykin et al., 2020).

Funding acquisition: Cameron R. Homeyer, Jessica B. Smith, Kristopher M. Bedka, Kenneth P. Bowman, David M. Wilmouth, Rei Ueyama, Jonathan M. Dean-Day, Jason M. St. Clair, Reem Hannun, David S. Sayres, Thomas F. Hanisco
Investigation: Cameron R. Homeyer, Kristopher M. Bedka, Andrea E. Gordon, Emily N. Tinney
Methodology: Cameron R. Homeyer, Kristopher M. Bedka
Project Administration: Cameron R. Homeyer, Kenneth P. Bowman
Software: Cameron R. Homeyer
Validation: Kristopher M. Bedka
Visualization: Cameron R. Homeyer
Writing – original draft: Cameron R. Homeyer
Writing – review & editing: Jessica B. Smith, Kristopher M. Bedka, Kenneth P. Bowman, David M. Wilmouth, Rei Ueyama, Jonathan M. Dean-Day, Jason M. St. Clair, Reem Hannun, Jennifer Hare, Apoorva Pandey, David S. Sayres, Thomas F. Hanisco, Andrea E. Gordon, Emily N. Tinney

Existing estimates of the contribution of tropopause-overshooting convection to the LS H_2O budget are based on observations of storms coupled with trajectory calculations driven by large-scale winds or on output from convection-resolving model simulations and vary from 10%–15% globally to 30%–45% regionally (e.g., Dauhut & Hohenegger, 2022; Dessler & Sherwood, 2004; Hanisco et al., 2007; Tinney & Homeyer, 2021; Ueyama et al., 2023). Most existing efforts to compute global LS H_2O budgets consider only the effects from tropical convection, but it is increasingly recognized that midlatitude overshooting convection is both deep and frequent (S. M. Khaykin et al., 2022; Liu & Liu, 2016; Liu et al., 2020; Werner et al., 2020). Thus, existing estimates of convection's contribution to LS H_2O are likely underestimates.

Improving our understanding of convective impacts on the LS H_2O budget was a primary objective of the recently-completed NASA Dynamics and Chemistry of the Summer Stratosphere (DCOTSS) field campaign. DCOTSS targeted the central U.S., which is a global hotspot for deep, midlatitude tropopause-overshooting convection (Liu et al., 2020). By combining near-real-time radar and satellite observations of storm top heights with trajectory forecasts, DCOTSS targeted convectively influenced stratosphere air within 3 days of occurrence. Additional layers impacted by overshooting convection at time periods beyond 3 days were also fortuitously sampled.

Past records of stratospheric heights hydrated by convection are based on aircraft and balloon observations. There are numerous metrics of stratospheric height that can be considered, including: (a) absolute altitude, (b) tropopause-relative altitude, (c) potential temperature (a measure of the energy required to lift tropospheric air into the stratosphere), and (d) O_3 mixing ratio, which increases rapidly above the tropopause (and typically ranges from 100 to 300 ppbv near the tropopause). Based on a comprehensive search of the literature, the two most extreme documented heights of stratospheric hydration by convection are one at 18.3 km altitude encountered during the SCOUT-AMMA aircraft campaign over Africa (S. Khaykin et al., 2009), and one at 430-K potential temperature (~800 ppbv O_3) encountered during the Aura Validation Experiment (AVE) aircraft campaign over the United States (Anderson et al., 2012; Hanisco et al., 2007; Smith et al., 2017). Tropopause-relative altitude records are unknown or uncertain based on documented events. All existing records were set in high-tropopause (i.e., tropical) environments, while the O_3 record from AVE has not been specified in prior work. Notable extremes in low-tropopause, midlatitude environments are those found in the recent Modular Observations Solutions of Earth Systems balloon campaign over Europe—14.25 km altitude, 375-K potential temperature, and ~650 ppbv O_3 (Khordakova et al., 2022). While all these listed extremes are based on in-situ observations, remotely sensed (lidar) data have provided indirect evidence of convective hydration (in the form of lofted ice) to even higher altitudes—up to 19.9 km (e.g., see Iwasaki et al., 2015), but this does not guarantee hydration since the ice particles may sediment before sublimating (Corti et al., 2008).

The existing records for in situ observations of the height of stratospheric hydration by convection were equaled or exceeded during DCOTSS. In this study, we briefly summarize the heights of hydration observed during the campaign and highlight the most extreme event sampled. These observations demonstrate the significant impacts of midlatitude tropopause-overshooting convection on LS H_2O, especially over the United States, and motivate renewed focus on their global impact.

2. Data and Methods

All data analyzed are sourced from the airborne, remote sensing, and model collections of the DCOTSS archive (NASA, 2023a, 2023b, 2023c). DCOTSS was a multi-year mission based predominantly out of Salina, Kansas in the central U.S., near the climatological maximum in the frequency of tropopause-overshooting convection (Cooney et al., 2018; Homeyer & Bowman, 2021). DCOTSS employed the NASA ER-2 aircraft, equipped with 12 instruments to measure atmospheric trace gas and aerosol composition and additional meteorological variables, spanning altitudes from the surface up to ~21.25 km above mean sea level (AMSL). Two multi-month deployments in 2021 and 2022 resulted in up to 29 flights with research-quality data, depending on the instrument.

2.1. Aircraft Observations

In-situ observations at 1-s intervals from three DCOTSS instruments are used to report upon extreme altitudes of stratospheric H_2O enhancements from convection. For stratospheric H_2O, data from the Harvard Herriott Hygrometer (HHH) within the Harvard Water Vapor instrument are used. HHH is a tunable diode laser direct

absorption sensor that provides H_2O mixing ratios with a precision of 0.1 ppmv and an accuracy of 10% (Sargent et al., 2013). Global Positioning System (GPS) altitudes and potential temperature are sourced from the Meteorological Measurement System (MMS) instrument. The MMS GPS altitudes have an accuracy of 15 m and potential temperature has an accuracy that ranges from ±0.5 K near the tropopause (~200 hPa) to ±1.5 K at the maximum ER-2 flight altitude (~50 hPa; Scott et al., 1990). Finally, O_3 mixing ratios are sourced from the Rapid OZone Experiment (ROZE). ROZE is a cavity-enhanced ultraviolet absorption instrument that measures O_3 at a precision of 1 ppbv and an accuracy of 6% (Hannun et al., 2020).

2.2. Environmental Assimilations

Hourly global assimilations of the atmospheric state from the fifth generation of the European Center for Medium-range Weather Forecasts reanalysis, ERA5 (Hersbach et al., 2020), are used for tropopause identification and trajectory calculations in this study. ERA5 volumes were obtained on a 0.25° latitude-longitude grid and 37 unevenly spaced pressure levels. The lapse-rate tropopause (LRT) definition (World Meteorological Organization, 1957) is applied to ERA5 vertical profiles after cubic spline interpolation to a regular 200 m grid. The resulting uncertainty in tropopause altitude is ≤250 m (e.g., Hoffmann & Spang, 2022). The LRT altitudes are interpolated linearly in space and time to the aircraft location and to the radar (Section 2.3) and satellite (Section 2.4) grids for analysis. Note that while ERA5 output is available on the full 137-level model grid, such data provide minimal refinement over the analyses provided herein.

2.3. Radar Observations

For high-resolution analyses of observed convection across the contiguous U.S. (CONUS), version 4.2 Gridded NEXRAD WSR-88D Radar (GridRad) data at 10-min intervals are used (Homeyer & Bowman, 2022). GridRad merges individual NEXRAD WSR-88D volumes onto a common grid with ~0.02° latitude-longitude resolution (~2-km) and 0.5-km altitude spacing below 7 km AMSL and 1-km spacing at higher altitudes up to 22 km AMSL. The GridRad domain spans 24–50°N latitude and 235–294°E longitude. The radar reflectivity at horizontal polarization Z_H is used to identify tropopause-overshooting convection as $Z_H = 10$ dBZ echo-top altitudes above the tropopause, applying a few quality-assurance criteria consistent with past GridRad overshoot climatologies (Cooney et al., 2018; Homeyer & Bowman, 2021; D. L. Solomon et al., 2016). As has been demonstrated in previous studies, GridRad echo-top altitudes are unbiased and have an uncertainty of ±1 km.

2.4. Satellite Observations

Radar-based overshoot detection over the CONUS is complemented by more extensive overshoot detection from Geostationary Observing Earth Satellite (GOES) imagery over North America. Cloud top height retrievals based on infrared (IR) GOES imagery are available at 10-min intervals during the 2021 and 2022 DCOTSS deployments, spanning a domain from 12 to 52°N latitude and 225–295°E longitude at 2-km horizontal resolution, and based on the method outlined in Griffin et al. (2016). In contrast to convection below the tropopause, IR brightness temperatures for overshooting convection are typically colder than the LS temperature. This inhibits the traditional cloud top height assignment approach of matching an IR temperature to a local tropospheric temperature profile. Cloud top height assignments here use an assumed lapse rate of 3.25 K km^{-1} above the tropopause. This lapse rate is smaller than that determined in Griffin et al. (2016) from a database of 1-km resolution Moderate Resolution Imaging Spectroradiometer and CloudSat overshooting observations and is required due to the larger pixel sizes of the GOES imagery used here. Corrections for parallax displacement errors are made prior to analysis.

In addition to cloud top height retrievals based on tropopause-relative IR cloud top temperature, we include 10-min stereoscopic cloud top height retrievals based on overlapping GOES-East and GOES-West IR imagery. Stereoscopic retrievals leverage the differential parallax shifts resulting from the different viewing angles of two satellites to determine cloud top heights with high fidelity and an accuracy that depends on the spatial resolution of the imagery (Fujita, 1982; Hasler et al., 1991; Mack et al., 1983; Negri, 1982). The IR stereoscopic cloud top heights retrieved for this study have an estimated uncertainty of 0.4 km (Podglajen et al., 2022). For the extreme event on the evening of 23 June 2022, 1-min stereo retrievals from overlapping mesoscale domains were also produced, but these unfortunately cut off directly downwind of the area of extreme overshooting. As a result,

Table 1
Extreme Altitudes Z, Tropopause-Relative Altitudes Z_{rel}, Potential Temperature θ, O_3, and H_2O Within DCOTSS (Dynamics and Chemistry of the Summer Stratosphere) Samples of Stratospheric Hydration by Convection

Flight date	Z (km)	Z_{rel} (km)	θ (K)	O_3 (ppbv)	H_2O (ppmv)
23 July 2021	17.02	2.4	402	373	5.2 (4.5)
26 July 2021	17.89	2.7	421	518	5.7 (4.0)
29 July 2021	17.93	3.3	433	668	7.4 (3.7)
02 August 2021	17.87	3.0	414	–	4.6 (4.0)
10 August 2021	17.58	3.4	424	483	9.1 (4.3)
14 August 2021	17.51	4.1	429	645	4.8 (4.0)
17 August 2021	16.38	0.9	390	298	5.8 (5.0)
19 August 2021	16.79	2.1	399	390	5.5 (5.0)
26 May 2022	14.17	1.2	386	269	7.8 (6.1)
29 May 2022	14.51	1.6	379	507	4.9 (4.2)
31 May 2022	17.25	2.4	414	790	11.7 (4.0)
02 June 2022	17.52	3.1	423	660	5.1 (3.8)
08 June 2022	17.67	3.7	424	693	16.1 (4.2)
10 June 2022	18.46	3.2	434	939	5.3 (4.1)
21 June 2022	17.73	3.6	429	920	5.4 (4.6)
24 June 2022	**19.26**	**4.1**	**463**	**1552**	5.7 (4.5)
27 June 2022	18.36	2.9	433	943	4.9 (4.3)
11 July 2022	17.63	1.9	413	493	4.7 (4.2)

Note. The O_3 and H_2O extremes are maximum values within 100 m of the identified Z maximum, with background H_2O mixing ratios in parentheses. Maximum values of each stratospheric height metric are emboldened.

only the 10-min stereo retrievals for the full analysis domain are shown, but the extent of altitude extremes and the maximum altitude observed utilize the 1-min analysis.

2.5. Trajectory Analyses

To link radar- and satellite-observed tropopause-overshooting convection to the aircraft measurements, we use 5-day forward isentropic trajectory calculations initialized in overshoot volumes and computed using the TRAJ3D model (Bowman, 1993; Bowman & Carrie, 2002; Bowman et al., 2013). Overshoot volumes are identified using a combination of storm-top heights and ERA5 LRT altitudes. For each overshoot, particles are initialized every 0.02° latitude-longitude and 500-m altitude from 500 m above the LRT altitude to the storm top and modified with up to ±0.01° latitude-longitude and up to ±250-m altitude uniformly-distributed random noise to better fill the volume. For a typical instantaneous radar-observed overshoot area of 40 km^2 (Cooney et al., 2018), the number of particles per 500-m altitude of overshooting is 10. Trajectory particles are advected forward 5 days using 2-D isentropic hourly wind fields from ERA5. Trajectory positions are saved hourly, with interpolation of particle positions in time for matching with the paths of the DCOTSS flights.

Trajectories are matched with a flight observation if they fall within a specified distance. This distance is determined from assumed time-dependent horizontal displacement errors resulting from numerical error of the trajectory calculation and ERA5 wind field errors, which we set somewhat conservatively here as 25 km per day. Time series measurements from each flight are then compared with matched trajectory counts to identify stratospheric H_2O enhancements linked to recent convection. We require H_2O enhancements to reach at least 0.5 ppmv above the adjacent background mixing ratio (i.e., the value before/after the enhancement at a similar altitude) and be broadly coincident with a substantial number of overshoot trajectory particles (≥20) to be classified as convection-driven hydration events.

3. Results

3.1. DCOTSS Altitude Extremes

Stratospheric H_2O enhancements linked to convection are found in observations from at least 18 DCOTSS flights, with the total sampling time in enhancements exceeding 28 hr (at least 20× more than all known in situ samples prior to DCOTSS). The highest stratospheric heights within these enhancements are listed in Table 1. The maximum H_2O mixing ratio at the extreme altitude is also listed, as well as the adjacent unperturbed background H_2O mixing ratio. Together, these measurements indicate that observed H_2O enhancements at altitude extremes range from 1.1 to 3.8× background, with an average enhancement of 1.55×. In comparison, DCOTSS measurements of convective enhancements of H_2O at altitudes closer to the tropopause routinely exceed 2× background and were up to 8× background (not shown). These extremes also reveal that convection-driven stratospheric hydration measured during DCOTSS extends well into the overworld stratosphere (potential temperature >380 K) on all but one flight. In fact, 18.5 of the 28.4 hr spent measuring convective hydration events during DCOTSS (~65%) were completed in the overworld. Comparatively, all stratospheric measurements from DCOTSS span 136.4 hr, 88% of which were in the overworld.

Previous records of the height of stratospheric enhancements were exceeded during either 3 or 4 DCOTSS flights, depending on the metric considered. Specifically, past altitude extremes were exceeded during the 10 June 2022, 24 June 2022, and 27 June 2022 flights, past potential temperature extremes were exceeded on the same three flights and the 29 July 2021 flight, and past O_3 mixing ratio extremes were exceeded on the 10 June 2022, 21 June 2022, 24 June 2022, and 27 June 2022 flights. Notably, all records were broken by a wide margin during the 24 June 2022 flight. This flight is the focus of the remaining analysis.

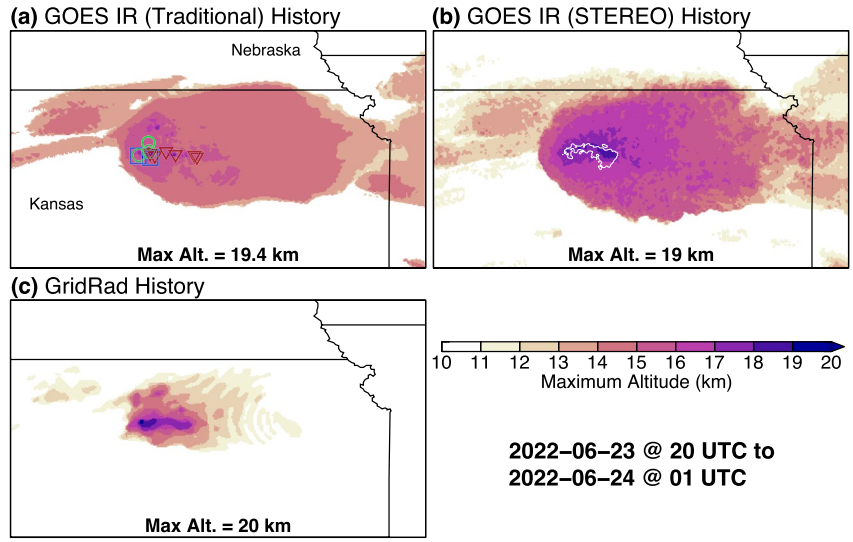

Figure 1. Storm top altitude history from (a) 10-min traditional Geostationary Observing Earth Satellite (GOES) infrared (IR) retrieval, (b) 10-min GOES IR stereoscopy, and (c) 10-min GridRad Z_H = 10 dBZ echo tops. Each panel shows the maximum altitude observed during a 5-hr period from 20 UTC on 23 June 2022 to 01 UTC on 24 June 2022 over a domain spanning 259–266°E and 37–41°N. Tornado, hail, and wind reports from the NCEI Storm Event Database are shown in (a) by the red triangles, green circles, and blue squares, respectively. The white contour in (b) outlines exceedances of 18 km from the 1-min stereoscopic retrievals. The storm-maximum altitudes observed by each data set are also indicated.

3.2. The 24 June 2022 DCOTSS Flight

The 24 June 2022 flight was designed with two primary targets: (a) stratospheric outflow from a deep, long-lived tornadic supercell storm that impacted north-central Kansas on the evening of 23 June 2022, and (b) stratospheric outflow from forecast storms in the Dakotas during the afternoon of 24 June 2022. Both targets were successfully sampled, but analysis herein focuses on the first target—responsible for the most extreme heights of stratospheric hydration sampled during DCOTSS. A map of the entire flight path is shown in Figure S1 in Supporting Information S1.

The 23 June 2022 supercell storm formed in north-central Kansas near 20 UTC and spawned 6 tornadoes as well as multiple hail and wind reports during the ~5 hr of its lifecycle (NCEI/NOAA, 2023). Its early development was characterized by explosive growth to altitudes of up to 20 km AMSL (up to 5 km above the environmental LRT height of ~15 km), followed by a sustained period (~1.5 hr) of exceptional height (≥19 km) and slow decay thereafter. Figure 1 shows extreme storm top heights from the GOES and GridRad products, accumulated over 5 hr, during the lifecycle of the Kansas supercell. Each storm-top height detection method indicates that the storm reached altitudes of at least 19 km, with a broad east-west oriented swath exceeding 17 km. Because the GOES products measure the cloud top and the GridRad products measure large precipitation particles, the areal expanse of extreme altitudes is greater for the GOES products. The Supporting Information S1 includes example vertical cross-sections of GridRad Z_H for the Kansas supercell during its deepest periods (Figures S2 and S3 in Supporting Information S1), corresponding GOES-East IR and visible imagery at one of the GridRad times (Figure S4 in Supporting Information S1), and a 1-min animation of GOES-East visible imagery for the storm's lifecycle.

The 24 June 2022 flight began at 17:52 UTC, ~20 hr after the deepest overshooting in the Kansas supercell storm. Based on near-real-time GridRad and GOES products, sampling of the stratospheric hydration was designed to bisect the forecast overshoot plume, which was being vertically tilted by environmental wind shear. In particular, the lowest part of the plume was being advected to the east, while the highest part was being advected to the west. A racetrack pattern oriented northwest to southeast over northern Kansas was designed to sample incrementally from ~18.4 km to ~19.25 km altitude in approximately 300-m increments. The second loop of the racetrack at the two highest altitudes was restricted to a shorter east-west distance, during which the plane ascended to a higher altitude than planned during the 18.95-km leg for a brief time. Marginal enhancements in stratospheric H_2O were observed during the first racetrack at the two lowest altitudes, while more substantial enhancements of up to ~1.2 ppmv (26%) above background were observed at the two highest altitudes during the second racetrack (Figure 2).

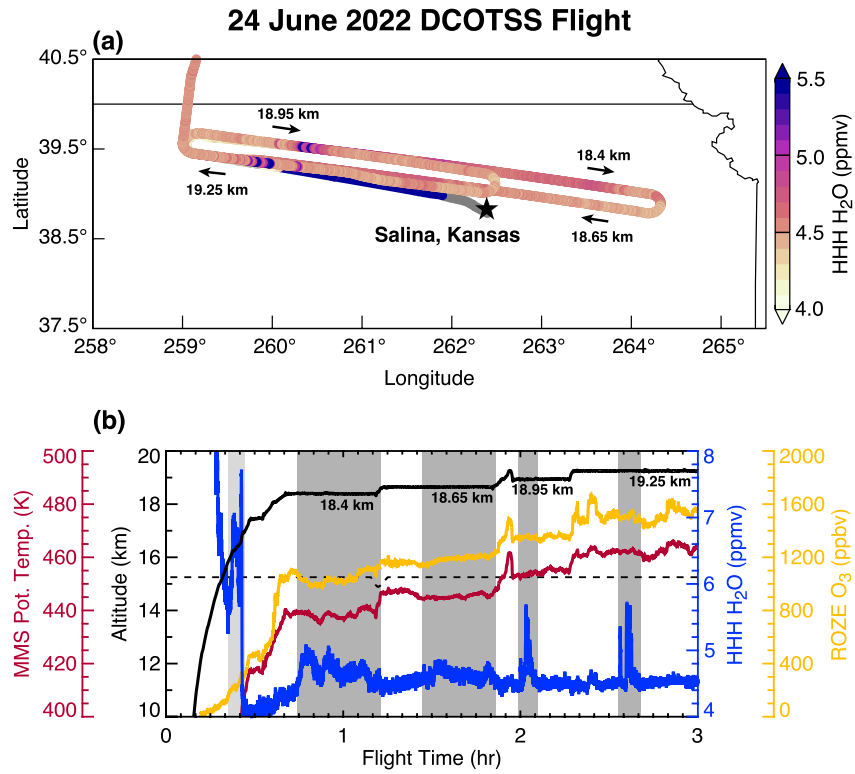

Figure 2. The first 3 hr of the Dynamics and Chemistry of the Summer Stratosphere (DCOTSS) 24 June 2022 flight track shown as (a) a map encompassing northern Kansas, colored by H_2O mixing ratio, and (b) a time series of Harvard Herriott Hygrometer (HHH) H_2O mixing ratio (blue), Rapid OZone Experiment (ROZE) O_3 mixing ratio (yellow), Meteorological Measurement System (MMS) Global Positioning System altitude (black), MMS potential temperature (red), and the ERA5 lapse-rate tropopause (LRT) altitude (dashed black line). The altitudes of each half segment of the two completed racetrack maneuvers are indicated in each panel, and the location of Salina, Kansas is indicated by the black star in (a). The light gray color-filled segment in (b) indicates a stratospheric H_2O enhancement linked to nearly 5-day-old convection, while each of the dark gray color-filled segments indicate stratospheric H_2O enhancements linked to the 23 June 2022 Kansas supercell.

Figure 2b shows a time series of the first 3 hr of the 24 June 2022 flight including HHH H_2O measurements, ROZE O_3, and MMS altitude and potential temperature. During initial ascent, the aircraft crossed the tropopause at an altitude of ~15.2 km (based on ERA5 reanalysis), where H_2O decreased as O_3 increased. At an altitude of ~16 km, the decrease in H_2O was briefly interrupted by an enhancement that extended up to ~17 km. This enhancement was trajectory-linked to GridRad- and GOES-observed convection that occurred nearly 5 days prior (not shown). Following this brief enhancement, H_2O concentrations dropped to background levels of 4–4.5 ppmv during the remainder of the ascent to the first racetrack leg at 18.4 km. During each pass of the racetrack maneuvers, marginal to moderate enhancements in H_2O were observed, each of which was trajectory-linked to the 23 June 2022 supercell storm. As previously highlighted, the enhancements were greatest at the two highest altitude passes. While H_2O perturbations were clear, O_3 and potential temperature were minimally changed within the outflow, except for perhaps at the lowest altitude sampled (18.4 km). Each of the four passes targeting the stratospheric H_2O enhancements from the 23 June 2022 supercell storm exceeded prior in-situ altitude, potential temperature, and O_3 extremes of observed convective hydration.

Finally, to visually demonstrate our trajectory-based linkage of the observed stratospheric H_2O enhancements with the Kansas supercell, we show overshoot trajectory positions at the approximate mid-time of the racetrack sampling and the 24 June 2022 flight track in Figure 3. In this case, only GridRad overshoot trajectory particles initialized during the prior 24-hr period are shown, with particles from the Kansas supercell storm in red and all other storms in black. Trajectories from older convection are not shown because they are more diffuse and do not alter the interpretation of the enhancements measured during the racetrack maneuvers. Comparing Figures 2a and 3 reveals a close coincidence between the orientation of the Kansas supercell overshoot plume

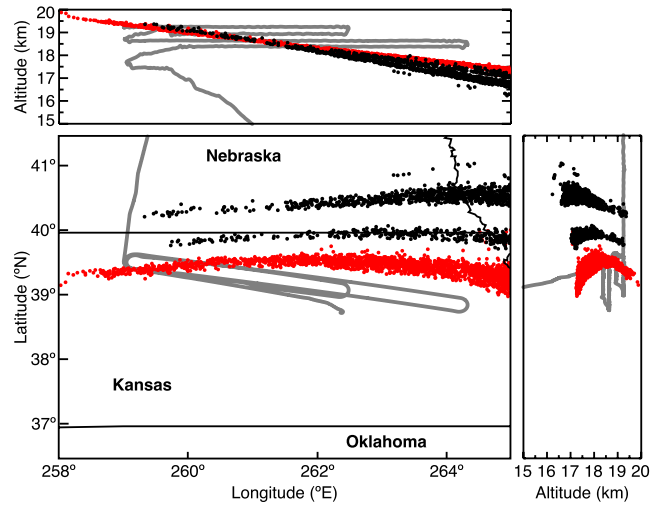

Figure 3. Snapshot of GridRad overshoot trajectory particles initialized in the 24-hr period prior to the 24 June 2022 flight at the approximate mid-time of sampling (valid 19 UTC on 24 June 2022). The large panel is a map extending from northern Oklahoma to central Nebraska, while the smaller panels at the top and right are longitude-altitude and latitude-altitude plots. In each panel, trajectory particles initialized in overshoots from the 23 June 2022 Kansas supercell are in red and all other storms in black. The ER-2 flight path is superimposed in gray.

and the observed H_2O enhancements, especially during the higher-altitude racetrack. The marginal enhancements observed during the first racetrack are consistent with a greater spatial offset between the aircraft and the radar-based overshoot plume at those altitudes. Lastly, the trajectory analysis demonstrates clearly that the Kansas supercell storm is likely the only storm responsible for the observed extreme altitudes of stratospheric hydration during the 24 June 2022 flight (since all other overshoot particles are displaced farther from the flight path).

4. Conclusions

DCOTSS measurements of stratospheric hydration establish new bounds for the impact of midlatitude convection on the stratospheric H_2O budget. Past evidence for extreme altitudes of H_2O enhancement were frequently met and greatly exceeded during DCOTSS (Table 1), with routine impacts to the overworld stratosphere (long thought to be minimally impacted by convection). While the most extreme event sampled during DCOTSS was highlighted here, many of the events sampled are of interest due to their size, duration, age, or more extensive chemical impacts (see scale discussion in Supporting Information S1). It is important to note that, while the highlighted extreme 23 June 2022 Kansas supercell results in significant increases to stratospheric H_2O at altitudes up to 19.25 km, such storms are rare, with only 10–100 per year reaching similar altitudes in the CONUS (Cooney et al., 2018). Based on DCOTSS sampling, overshooting convection does routinely hydrate the stratosphere up to altitudes of ∼18 km, tropopause-relative altitudes of 3 km, potential temperatures of 420 K, and O_3 mixing ratios of ∼500 ppbv. However, it is not appropriate to estimate the absolute frequency of convective hydration of the stratosphere from aircraft data alone due to sampling biases arising from targeted observation. Rather, these measurements and the growing body of literature identifying the global significance of midlatitude tropopause-overshooting convection frequency and height motivate increased consideration of its impact on the stratospheric H_2O budget.

Data Availability Statement

All DCOTSS aircraft (NASA, 2023a), radar & satellite (NASA, 2023c), and trajectory (NASA, 2023b) data analyzed here are available from the NASA Atmospheric Sciences Data Center. The GOES IR stereoscopic retrievals are available online from NASA Langley: https://science-data.larc.nasa.gov/LaRC-SD-Publications/2023-05-23-001-KMB/.

Acknowledgments
We thank the entire DCOTSS team for enabling the successful flights and measurements reported upon here. All authors were supported by the National Aeronautics and Space Administration (NASA) under Earth Venture Suborbital-3 program awards for DCOTSS (80NSSC19K0347, 80NSSC19K0326, 80NSSC19K0341).

References

Anderson, J. G., Wilmouth, D. M., Smith, J. B., & Sayres, D. S. (2012). UV dosage levels in summer: Increased risk of ozone loss from convectively injected water vapor. *Science*, *337*(6096), 835–839. https://doi.org/10.1126/science.1222978

Banerjee, A., Chiodo, G., Previdi, M., Ponater, M., Conley, A. J., & Polvani, L. M. (2019). Stratospheric water vapor: An important climate feedback. *Climate Dynamics*, *53*(3–4), 1697–1710. https://doi.org/10.1007/s00382-019-04721-4

Bowman, K. P. (1993). Large-scale isentropic mixing properties of the Antarctic polar vortex from analyzed winds. *Journal of Geophysical Research*, *98*(D12), 23013–23027. https://doi.org/10.1029/93JD02599

Bowman, K. P., & Carrie, G. D. (2002). The mean-meridional transport circulation of the troposphere in an idealized GCM. *Journal of the Atmospheric Sciences*, *59*(9), 1502–1514. https://doi.org/10.1175/1520-0469(2002)059<1502:TMMTCO>2.0.CO;2

Bowman, K. P., Lin, J. C., Stohl, A., Draxler, R., Konopka, P., Andrews, A., & Brunner, D. (2013). Input data requirements for Lagrangian trajectory models. *Bulletin America Meteorology Social*, *94*(7), 1051–1058. https://doi.org/10.1175/BAMS-D-12-00076.1

Brewer, A. W. (1949). Evidence for a world circulation provided by the measurements of helium and water vapour distribution in the stratosphere. *Quarterly Journal of the Royal Meteorological Society*, *75*(326), 351–363. https://doi.org/10.1002/qj.49707532603

Cooney, J. W., Bowman, K. P., Homeyer, C. R., & Fenske, T. M. (2018). Ten-year analysis of tropopause-overshooting convection using GridRad data. *Journal of Geophysical Research: Atmospheres*, *123*(1), 329–343. https://doi.org/10.1002/2017JD027718

Corti, T., Luo, B. P., de Reus, M., Brunner, D., Cairo, F., Mahoney, M. J., et al. (2008). Unprecedented evidence for deep convection hydrating the tropical stratosphere. *Geophysical Research Letters*, *35*, L10810. https://doi.org/10.1029/2008GL033641

Dauhut, T., & Hohenegger, C. (2022). The contribution of convection to the stratospheric water vapor: The first budget using a global storm-resolving model. *Journal of Geophysical Research: Atmospheres*, *127*(5), e2021JD036295. https://doi.org/10.1029/2021JD036295

Del Genio, A. D., Yao, M.-S., & Jonas, J. (2007). Will moist convection be stronger in a warmer climate? *Geophysical Research Letters*, *34*(16), L16703. https://doi.org/10.1029/2007GL030525

Dessler, A. E., & Sherwood, S. C. (2004). Effect of convection on the summertime extratropical lower stratosphere. *Journal of Geophysical Research*, *109*(D23), D23301. https://doi.org/10.1029/2004JD005209

Forster, P. M. F., & Shine, K. P. (1999). Stratospheric water vapour changes as a possible contributor to observed stratospheric cooling. *Geophysical Research Letters*, *26*(21), 3309–3312. https://doi.org/10.1029/1999GL010487

Fujita, T. T. (1982). Principle of stereoscopic height computations and their applications to stratospheric cirrus over severe thunderstorms. *Journal of the Meteorological Society of Japan*, *60*(1), 355–368. https://doi.org/10.2151/jmsj1965.60.1_355

Gensini, V. A., & Mote, T. L. (2015). Downscaled estimates of late 21st century severe weather from CCSM3. *Climatic Change*, *129*(1–2), 307–321. https://doi.org/10.1007/s10584-014-1320-z

Griffin, S. M., Bedka, K. M., & Velden, C. S. (2016). A method for calculating the height of overshooting convective cloud tops using satellite-based IR imager and *cloudsat* cloud profiling radar observations. *Journal of Applied Meteorology and Climatology*, *55*(2), 479–491. https://doi.org/10.1175/JAMC-D-15-0170.1

Hanisco, T. F., Moyer, E. J., Weinstock, E. M., Clair, J. M. S., Sayres, D. S., Smith, J. B., et al. (2007). Observations of deep convective influence on stratospheric water vapor and its isotopic composition. *Geophysical Research Letters*, *34*(4), L04814. https://doi.org/10.1029/2006GL027899

Hannun, R. A., Swanson, A. K., Bailey, S. A., Hanisco, T. F., Bui, T. P., Bourgeois, I., et al. (2020). A cavity-enhanced ultraviolet absorption instrument for high-precision, fast-time-response ozone measurements. *Atmospheric Measurement Techniques*, *13*(12), 6877–6887. https://doi.org/10.5194/amt-13-6877-2020

Hasler, A. F., Strong, J., Woodward, R. H., & Pierce, H. (1991). Automatic analysis of stereoscopic satellite image pairs for determination of cloud-top height and structure. *Journal of Applied Meteorology*, *30*(3), 257–281. https://doi.org/10.1175/1520-0450(1991)030<0257:AAOSSI>2.0.CO;2

Hersbach, H., Bell, B., Berrisford, P., Hirahara, S., Horányi, A., Muñoz-Sabater, J., et al. (2020). The ERA5 global reanalysis. *Quarterly Journal of the Royal Meteorological Society*, *146*(730), 1999–2049. https://doi.org/10.1002/qj.3803

Hoffmann, L., & Spang, R. (2022). An assessment of tropopause characteristics of the ERA5 and ERA-Interim meteorological reanalyses. *Atmospheric Chemistry and Physics*, *22*(6), 4019–4046. https://doi.org/10.5194/acp-22-4019-2022

Homeyer, C. R., & Bowman, K. P. (2021). A 22-year evaluation of convection reaching the stratosphere over the United States. *Journal of Geophysical Research: Atmospheres*, *126*(13), e2021JD034808. https://doi.org/10.1029/2021JD034808

Homeyer, C. R., & Bowman, K. P. (2022). Algorithm description document for version 4.2 of the three-dimensional gridded NEXRAD WSR-88D radar (GridRad) dataset (Tech. Rep.). Retrieved from http://gridrad.org

Iwasaki, S., Luo, Z. J., Kubota, H., Shibata, T., Okamoto, H., & Ishimoto, H. (2015). Characteristics of cirrus clouds in the tropical lower stratosphere. *Atmospheric Research*, *164–165*, 358–368. https://doi.org/10.1016/j.atmosres.2015.06.009

Khaykin, S., Legras, B., Bucci, S., Sellitto, P., Isaksen, L., Tencé, F., et al. (2020). The 2019/20 Australian wildfires generated a persistent smoke-charged vortex rising up to 35 km altitude. *Communications Earth & Environment*, *22*(1), 22. https://doi.org/10.1038/s43247-020-00022-5

Khaykin, S., Pommereau, J.-P., Korshunov, L., Yushkov, V., Nielsen, J., Larsen, N., et al. (2009). Hydration of the lower stratosphere by ice crystal geysers over land convective systems. *Atmospheric Chemistry and Physics*, *9*(6), 2275–2287. https://doi.org/10.5194/acp-9-2275-2009

Khaykin, S. M., Moyer, E., Krämer, M., Clouser, B., Bucci, S., Legras, B., et al. (2022). Persistence of moist plumes from overshooting convection in the Asian monsoon anticyclone. *Atmospheric Chemistry and Physics*, *22*(5), 3169–3189. https://doi.org/10.5194/acp-22-3169-2022

Khordakova, D., Rolf, C., Grooß, J.-U., Müller, R., Konopka, P., Wieser, A., et al. (2022). A case study on the impact of severe convective storms on the water vapor mixing ratio in the lower mid-latitude stratosphere observed in 2019 over Europe. *Atmospheric Chemistry and Physics*, *22*(2), 1059–1079. https://doi.org/10.5194/acp-22-1059-2022

Le Texier, H., Solomon, S., & Garcia, R. R. (1988). The role of molecular hydrogen and methane oxidation in the water vapour budget of the stratosphere. *Quarterly Journal of the Royal Meteorological Society*, *114*(480), 281–295. https://doi.org/10.1002/qj.49711448002

Liu, N., & Liu, C. (2016). Global distribution of deep convection reaching tropopause in 1 year GPM observations. *Journal of Geophysical Research: Atmospheres*, *121*(8), 3824–3842. https://doi.org/10.1002/2015JD024430

Liu, N., Liu, C., & Hayden, L. (2020). Climatology and detection of overshooting convection from 4 years of GPM precipitation radar and passive microwave observations. *Journal of Geophysical Research: Atmospheres*, *125*(7), e2019JD032003. https://doi.org/10.1029/2019JD032003

Mack, R. A., Hasler, A. F., & Adler, R. F. (1983). Thunderstorm cloud top observations using satellite stereoscopy. *Monthly Weather Review*, *111*(10), 1949–1964. https://doi.org/10.1175/1520-0493(1983)111<1949:TCTOUS>2.0.CO;2

Millán, L., Santee, M. L., Lambert, A., Livesey, N. J., Werner, F., Schwartz, M. J., et al. (2022). The Hunga Tonga-Hunga Ha'apai hydration of the stratosphere. *Geophysical Research Letters*, *49*(13), e2022GL099381. https://doi.org/10.1029/2022GL099381

NASA. (2023a). *Dynamics and chemistry of the summer stratosphere airborne data products*. NASA Atmospheric Sciences Data Center. https://doi.org/10.5067/ASDC/DCOTSS-Aircraft-Data_1

NASA. (2023b). *Dynamics and chemistry of the summer stratosphere model output*. NASA Atmospheric Sciences Data Center. https://doi.org/10.5067/ASDC/DCOTSS-Model-Output_1

NASA. (2023c). *Dynamics and chemistry of the summer stratosphere radar and satellite (remote sensing) data products*. NASA Atmospheric Sciences Data Center. https://doi.org/10.5067/ASDC/DCOTSS-Radar-Satellite-Data_1

NCEI/NOAA. (2023). *NOAA's storm events database*. National Centers for Environmental Information. Retrieved from https://www.ncdc.noaa.gov/stormevents/

Negri, A. J. (1982). Cloud-top structure of tornadic storms on 10 April 1979 from rapid scan and stereo satellite observations. *Bulletin America Meteorology Social*, *63*(10), 1151–1159. https://doi.org/10.1175/1520-0477-63.10.1151

Podglajen, A., Le Pichon, A., Garcia, R. F., Gérier, S., Millet, C., Bedka, K., et al. (2022). Stratospheric balloon observations of infrasound waves from the 15 January 2022 Hunga eruption, Tonga. *Geophysical Research Letters*, *49*(19), e2022GL100833. https://doi.org/10.1029/2022GL100833

Romps, D. M., Seeley, J. T., Vollaro, D., & Molinari, J. (2014). Projected increase in lightning strikes in the United States due to global warming. *Science*, *346*(6211), 851–854. https://doi.org/10.1126/science.1259100

Sargent, M. R., Sayres, D. S., Smith, J. B., Witinski, M., Allen, N. T., Demusz, J. N., et al. (2013). A new direct absorption tunable diode laser spectrometer for high precision measurement of water vapor in the upper troposphere and lower stratosphere. *Review of Scientific Instruments*, *84*(7), 074102. https://doi.org/10.1063/1.4815828

Schwartz, M. J., Read, W. G., Santee, M. L., Livesey, N. J., Froidevaux, L., Lambert, A., & Manney, G. L. (2013). Convectively injected water vapor in the North American summer lowermost stratosphere. *Geophysical Research Letters*, *40*(10), 1–6. https://doi.org/10.1002/grl.50421

Scott, S. G., Bui, T. P., Chan, K. R., & Bowen, S. W. (1990). The meteorological measurement system on the NASA ER-2 aircraft. *Journal of Atmospheric and Oceanic Technology*, *7*(4), 525–540. https://doi.org/10.1175/1520-0426(1990)007<0525:TMMSOT>2.0.CO;2

Smith, J. B., Wilmouth, D. M., Bedka, K. M., Bowman, K. P., Homeyer, C. R., Dykema, J. A., et al. (2017). A case study of convectively sourced water vapor observed in the overworld stratosphere over the United States. *Journal of Geophysical Research: Atmospheres*, *122*(17), 9529–9554. https://doi.org/10.1002/2017JD026831

Solomon, D. L., Bowman, K. P., & Homeyer, C. R. (2016). Tropopause-penetrating convection from three-dimensional gridded NEXRAD data. *Journal of Applied Meteorology and Climatology*, *55*(2), 465–478. https://doi.org/10.1175/JAMC-D-15-0190.1

Solomon, S., Rosenlof, K. H., Portmann, R. W., Daniel, J. S., Davis, S. M., Sanford, T. J., & Plattner, G.-K. (2010). Contributions of stratospheric water vapor to decadal changes in the rate of global warming. *Science*, *327*(5970), 1219–1223. https://doi.org/10.1126/science.1182488

Tinney, E. N., & Homeyer, C. R. (2021). A 13-year trajectory-based analysis of convection-driven changes in upper troposphere lower stratosphere composition over the United States. *Journal of Geophysical Research: Atmospheres*, *126*(3), e2020JD033657. https://doi.org/10.1029/2020JD033657

Ueyama, R., Schoeberl, M., Jensen, E., Pfister, L., Park, M., & Ryoo, J.-M. (2023). Convective impact on the global lower stratospheric water vapor budget. *Journal of Geophysical Research: Atmospheres*, *128*(6), e2022JD037135. https://doi.org/10.1029/2022JD037135

Werner, F., Schwartz, M. J., Livesey, N. J., Read, W. G., & Santee, M. L. (2020). Extreme outliers in lower stratospheric water vapor over North America observed by MLS: Relation to overshooting convection diagnosed from colocated Aqua-MODIS data. *Geophysical Research Letters*, *47*(24), e2020GL090131. https://doi.org/10.1029/2020GL090131

World Meteorological Organization. (1957). Meteorology—A three-dimensional science: Second session of the commission for aerology. *World Meteorological Organization Bulletin*, *4*, 134–138.